

# On the nature of Off-pulse emission from pulsars

Rahul Basu<sup>1</sup>, Dipanjan Mitra<sup>1</sup> and Ramana Athreya<sup>2</sup>

<sup>1</sup>*National Centre for Radio Astrophysics, P. O. Bag 3, Pune University Campus, Pune: 411 007. India.*

<sup>2</sup>*Indian Institute of Science Education & Research (IISER) - Pune, 900, NCL Innovation Park, Homi Bhabha Road, Pune: 411 008. India.*

rbasu@ncra.tifr.res.in, dmitra@ncra.tifr.res.in, rathreya@iiserpune.ac.in

## ABSTRACT

In Basu et al. 2011 we reported the detection of Off-pulse emission from two long period pulsars B0525+21 and B2045-16. The pulsars were observed at a single epoch using the 325 MHz frequency band of the Giant Meterwave Radio Telescope (GMRT). In this paper we report a detailed study of the Off-pulse emission from these two pulsars using multiple observations at two different frequencies, 325 MHz and 610 MHz bands of GMRT. We report detection of Off-pulse emission during each observation and based on the scintillation effects and spectral index of Off-pulse emission we conclude a magnetospheric origin. The magnetospheric origin of Off-pulse emission gives rise to various interesting possibilities about its emission mechanism and raises questions about the structure of the magnetosphere.

*Subject headings:* pulsars: general – pulsars: individual (B0525+21, B2045-16) – techniques: interferometric

## 1. Introduction

The basic pulsar phenomenon where a series of highly regular narrow pulses is observed has been explained from the very outset by invoking the lighthouse model. In this model the highly magnetized, rotating neutron star has a charge filled magnetosphere. The magnetic field surrounding the central star is characterized by a dipolar field with open and closed field line regions. The locus of the foot prints of the open field lines on the neutron star surface constitute the polar cap. It is believed that plasma is accelerated to relativistic velocities at the polar cap, which streams out along the open field lines giving rise to the observed coherent radio emission. This originate a few hundred kilometers above the stellar surface, and appear as narrow pulses due to the rotation of the neutron star. The plasma remains trapped in the closed field line regions thereby abstaining from the emission process.

The known cases of emission from pulsars outside the main pulse are the interpulse, pre/post-cursor emission and the pulsar wind nebulae

(PWNe). The interpulse and pre/post-cursors emission appear as temporal structures in the time series data. The interpulse emission (located 180° away from main pulse) are usually associated with orthogonal rotators, the radio emission in the interpulse believed to originate from the opposite magnetic pole. The pre/post-cursor emission are located closer to the main pulse and connected via a bridge emission. They are highly polarized and their location in the magnetosphere is uncertain. The time series observations of pulsars are insensitive to any temporally constant background emission. The technique of gated interferometry, where the main pulse emission is blocked, can probe a constant background emission by mapping the Off-pulse region. In the past gated interferometric studies have been employed to detect PWNe from very energetic young pulsars with spindown energies  $\dot{E} \geq 10^{34}$  erg s<sup>-1</sup> (Frail & Scharringhausen 1997) .

In recent studies we reported the detection of off-pulse emission from two long period pulsars based on gated interferometric observations with the Giant Metrewave Radio Telescope (GMRT) at

325 MHz (Basu et al. 2011), (hereafter PaperI). Our detection of off-pulse emission is a ‘unique’ and surprising result because the two long period pulsars are relatively old and less energetic unlike the pulsars known to harbour PWN. Also the pulse profiles do not show any temporal structures outside the main pulse. We concluded on heuristic grounds that the detected Off-pulse emission is magnetospheric in origin based on outlandish expectations of ISM densities to sustain a PWM for these pulsar energetics.

In this paper we continue our previous investigations of Off-pulse emission. In section 2 we report the detection of Off-pulse emission at widely separated times and frequencies (see section 2.1) and also account for the authenticity of these detections by carrying out a detailed test of the instrument to weed out possibility of the detected emission being a result of smearing of the pulsed signal across time (see section 2.2). In section 3 we study the flux variations which lead us to an upper limit of the size of the Off-pulse emission region (see section 3.1) and we also obtain secure estimates of its spectral index  $\alpha$  (see section 3.2). Based on our estimates of these properties we conclude a magnetospheric origin for Off-pulse emission. Finally we discuss the results and their implications in section 4.

## 2. Observations & Analysis

### 2.1. Multi-epoch/ Multi-frequency observations

We reported detection of off-pulse emission in paperI from two pulsars PSR B0525+21 and B2045–16 based on single epoch observations at 325 MHz with the GMRT. We have now observed these two pulsars at 325 MHz and 610 MHz multiple times. The observations were carried out between January 2010 and August, 2011 (see table 1). The specialized interferometric high time resolutions of 128/256 milliseconds supported by the GMRT correlator system were used for these observations. We observed the pulsars at both 325 MHz and 610 MHz frequency band. During the early months of 2011 the GMRT correlator system was upgraded from the previously existing Hardware backend (GHB) to a Software backend (GSB) which is currently under use. The GHB was used with the lowest available time resolution

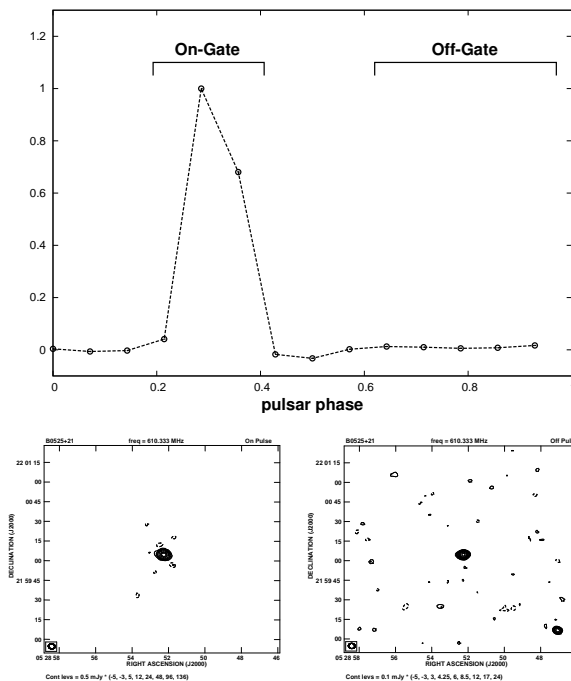


Fig. 1.— The folded profile (top) of B0525+21 representing the On- and Off-pulse gates. The corresponding contour maps of the On-pulse (bottom left) and Off-pulse (bottom right) emission from the pulsar. The data was recorded on 15 February, 2011 at 610 MHz.

Table 1: Observation details

Date	Pulsar	freq(chan) MHz	Time mins	time res msec	Corr	ang res "×"	On flux(rms) mJy	Off flux(rms) mJy	$\frac{Off}{On}$
18 Jan, 2010*	B0525+21	325(128)	160	261	GHB	9.5×6.5	30.0±2.1(0.55)	3.9±0.5(0.45)	0.130±0.026
08 Jul, 2011	B0525+21	325( 32)	240	250	GSB	8.3×6.7	44.5±2.4(0.65)	6.6±0.5(0.4)	0.148±0.019
09 Jul, 2011	B0525+21	325( 32)	120	250	GSB	10.0×7.4	48.2±2.6(0.7)	6.5±0.6(0.5)	0.135±0.020
15 Feb, 2011	B0525+21	610( 32)	330	250	GSB	4.8×4.0	21.1±1.5(0.45)	3.6±0.3(0.13)	0.171±0.026
22 Jul, 2011	B0525+21	610( 32)	240	250	GSB	5.4×3.7	20.0±1.2(0.65)	2.8±0.2(0.13)	0.140±0.018
16 Jan, 2010*	B2045-16	325(128)	180	131	GHB	11.9×7.2	110.5±7.9(2.1)	4.3±1.1(0.65)	0.039±0.013
03 Aug, 2011	B2045-16	325(256)	200	125	GSB	10.2×7.7	57.5±3.2(0.35)	6.8±0.4(0.2)	0.118±0.014
14 Feb, 2011	B2045-16	610(128)	180	131	GHB	5.8×4.3	23.9±1.7(1.0)	1.1±0.2(0.13)	0.046±0.012
25 Aug, 2011	B2045-16	610(256)	140	125	GSB	4.9×4.3	43.2±3.1(0.45)	4.6±0.3(0.11)	0.106±0.015

\* reported in Basu et al. 2011

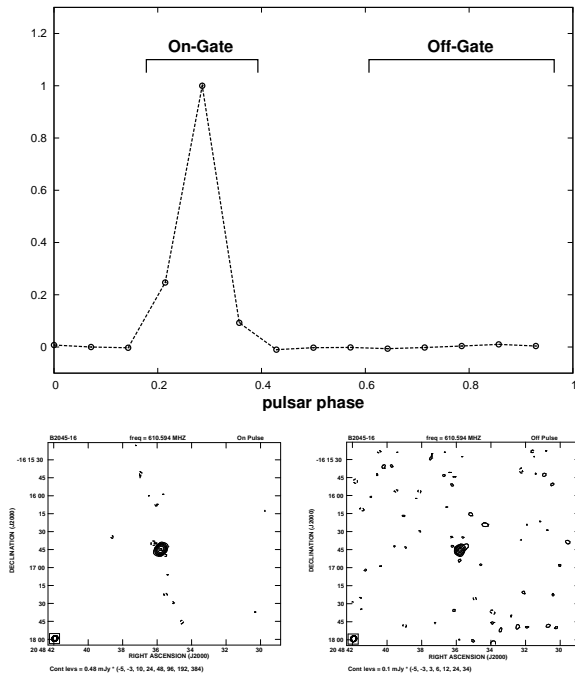


Fig. 2.— The folded profile (top) of B2045-16 representing the On- and Off-pulse gates. The corresponding contour maps of the On-pulse (bottom left) and Off-pulse (bottom right) emission from the pulsar. The data was recorded on 25 August, 2011 at 610 MHz.

of 131 msec and a bandwidth of 16 MHz split into 128 channels. The GSB initially operated at a lowest time resolution of 251 milliseconds over a 16 MHz bandwidth spread across 32 channels. The GSB was extended to operate at 125 milliseconds time resolution over 16 MHz bandwidth split into 256 channels. All these modes were used for our observations as documented in columns 1 to 6 of table 1.

We used the technique of ‘offline-gating’ discussed in paper I to image the On- and Off-pulse regions. To summarize briefly, the interferometric time series data was folded with the periodicity of the pulsar to determine the On- and Off-pulse phases; a phase was assigned to each time record and two ‘gates’ were put in to separate the On- and Off-phase data, which were then imaged and the flux of the point source coincident with the pulsar position in each image measured. To check for the consistency of measured pulsar flux over different epochs of observations we compared the flux of the other point sources in the field which were within 10% (within calibration errors) for all observations. This indicates that any large variations in the On- and Off-pulse flux were intrinsic effects.

Table 1 gives the details of the experimental setup and also summarizes the results of the analysis. Column 7 shows the angular resolution in the images. During each of these observations a point source was detected at the location of the pulsars in both the On- and Off-pulse maps. The On-pulse flux, averaged over the pulse period (all

On-pulse flux reported in this paper are averaged over the entire period), are reported in column 8 while column 9 report the measured Off-pulse flux. The ratio of the Off-pulse flux and period averaged On-pulse flux is shown in column 10. An example of Off-pulse and On-pulse image for a single epoch at 610 MHz is shown in figure 1 and 2.

Thus in summary, in each of the multi-epoch and multi-frequency interferometric observations we have detected off-pulse emission from PSR B0525+21 and B2045-16. In our studies we used two different correlator systems, the GHB and GSB, and two different frequency bands, 325 MHz and 610 MHz bands, which make it extremely unlikely for the Off-pulse to be a spurious detection.

## 2.2. Pulsed Noise Source: Smearing of signal across time.

In paperI, we discussed the possibility that off-pulse emission was a result of temporal leakage of the pulsed signal. To investigate this we recorded front end terminated 131 milliseconds interferometric data and estimated the autocorrelation of the noise signal for each baseline. We found that the observed autocorrelations were significantly lower (0.04%) than the required levels (around 1%) to explain the observed off-pulse emission (see paperI for details).

However, the above experiment did not account for temporal leakages due to a strong pulsed signal as seen in pulsars. In order to investigate this effect a series of narrow single pulses with no Off-pulse emission was required to be introduced in the receiver system. A broad-band pulsed noise source with a period of 4 seconds and a duty cycle of 32 millisecond was developed for this purpose. The power of the On-pulse signal was -5 dbm and the signal was down by 30 db in the Off-state, which was significantly below the detected Off-pulse emission. The noise source was radiated from an antenna in the central square of the GMRT. Interferometric data was recorded with a time resolution of 251 milliseconds for about half an hour with the noise source switched on. Since the noise source was in the near field, the geometrical delay calculations were vastly complicated (it is a function of the distance of the individual antennas from the pulsed noise source). We did not correct for any geometrical delay in the correlator chain. This implied that only for a handful of cases

(10 baselines) the antennas were close enough for the coherence condition to hold and these baselines were used for the subsequent analysis as discussed below.

If there was no leakage of the pulsed signal in time, the folded profile with increasing number of periods averaged together, for any baseline, would show a decrease in the off-pulse noise and an increase in the signal to noise ratio (SNR) by a factor  $\sqrt{N}$ , where N is the number of folded periods.

The interferometer measures the correlation between the voltages recorded by the individual elements (Thompson et al. 1986).

$$r(\tau) = \frac{1}{2T} \int_{-T}^T V_1(t) \times V_2(t - \tau) dt$$

where the quantity  $r(\tau)$  is related to the intensity of the incident signal and  $2T$  is the temporal resolution (251 msec).

We assume that the system introduces a constant fractional leakage  $\epsilon$  into the adjacent time bin (this is the most likely situation, besides any other situation will lead to a lower SNR). The correlation in the adjacent bin in such a scenario is given as:

$$r'(\tau) = \epsilon^2 \frac{1}{2T} \int_{-T}^T V_1(t) \times V_2(t - \tau) dt, \quad \epsilon < 1$$

The statistics of the bins adjacent to the pulsed source is characterized by a mean ( $\mu$ ) and rms ( $\sigma$ ) given as:

$$\mu = \epsilon^{2n} \frac{1 - \epsilon^{2N}}{N(1 - \epsilon^2)} \times r(\tau) \quad (1)$$

$$\sigma \sim \frac{\epsilon^{2n}}{(1 - \epsilon^2)} \sqrt{\frac{1}{N} \frac{1 - \epsilon^{2N}}{1 + \epsilon^2}} \times r(\tau) \quad (2)$$

Here the first bin is the  $n^{th}$  bin from the pulsed source with N bins used for statistics;  $r(\tau)$  is the correlation in the pulsed source bin. The statistics of the adjacent bins will be governed by a combination of gaussian statistics due to random noise and the constant leakage into adjacent bins. However for sufficient long averaging the effect of random noise will be overshadowed by the leakage term and the SNR for the pulsed source would saturate at a constant level.

The interferometric data from the pulsed noise source were folded with a periodicity of 4 seconds

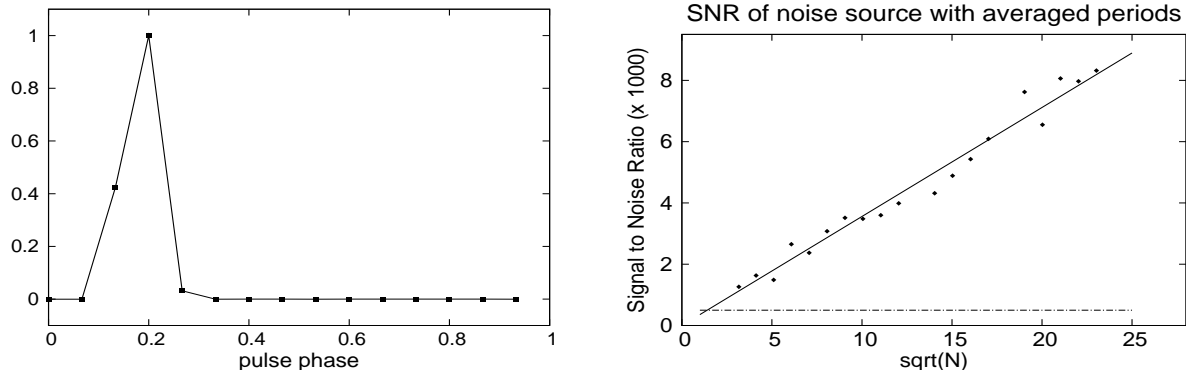


Fig. 3.— The pulsed noise source as observed with the interferometer (left), with 565 folded periods of 4 sec and a time resolution of 250 msec. The change in signal to noise ratio of the pulsed signal with increasing number of folded periods ( $N$ ) from 10 periods to 565 periods (right). The dark solid lines represent a linear increase of SNR with  $\sqrt{N}$  indicating the baseline to be noise like. The dot dashed horizontal line is the level at which the SNR was expected to saturate if temporal leakage was the source of Off-pulse emission.

to determine the profile (see fig 3). A large number of profiles of the noise source were generated by folding an increasing number of periods. The SNR for each of these profiles were calculated, by dividing the total signal in the noise bin with the rms fluctuation in the adjacent bins. In figure 3 we plot the SNR as a function of the square root of the number of periods (points) along with the best fit (dark solid line).

We have detected off-pulse emission in pulsars at a level of 0.5 – 1 % of the On-pulse flux. The Off-pulse region in our studies are 5 bins ( $n=5$ ) from the On-pulse and we can calculate the leakage ( $\epsilon$ ) required using equation 1 and 2 to explain the detected off-pulse. This would lead to a SNR  $\sim 500$ , as represented by the dot dashed horizontal line in figure 3. However the bins adjacent to the noise source continue to follow gaussian statistics at SNR  $\sim 8000$  as seen in figure 3. This implies that the temporal leakage can only lead to a Off-pulse emission which is less than 0.03% of the On-pulse flux. Hence the detected off-pulse emission cannot originate as a result of temporal leakage of the On-pulse signal into adjacent time bins.

The unprecedented detection of Off-pulse emission makes it imperative to exhaust all possibilities of spurious detection. In this section we report repeated detections of off-pulse emission in multiple epochs and frequencies using different correlator systems and also rule out spurious detection that can result due to temporal leakage. We have es-

tablished that the Off-pulse emission is genuine and not a result of systematic anomaly. We now look ahead to determining the nature of Off-pulse emission.

### 3. Magnetospheric origin of off-pulse: Flux Variation & Spectral Index study.

In paper I we argued that low energetic ( $\dot{E} \sim 10^{31}$  ergs/s) long period ( $\sim 2$  sec) pulsars B0525+21 and B2045-16, were unlikely to harbour PWNe around them. The ISM particle densities required to drive either a static or a bow shock nebula turns out to be grossly unrealistic. We concluded that the Off-pulse emission must have a magnetospheric origin.

The radio emission in PWNe is due to relativistic charged particles producing synchrotron emission in the ambient ISM magnetic field. The typical size of PWNe is between 0.1–1 parsec due to expansion of the pulsar wind in the surrounding ISM (Gaensler & Slane 2006). If the Off-pulse emission can be constrained to several orders of magnitude lower than the typical PWN sizes, a PWN origin can be discounted. Further a wide range of studies (Weiler & Sramek 1988) suggest that PWNe observed in the radio frequencies between 100 MHz to 10 GHz, are usually characterized by a flat radio spectral index  $\alpha$  in the range  $0 > \alpha > -0.5$  (where  $S \sim \nu^\alpha$ ). The spectrum pre-

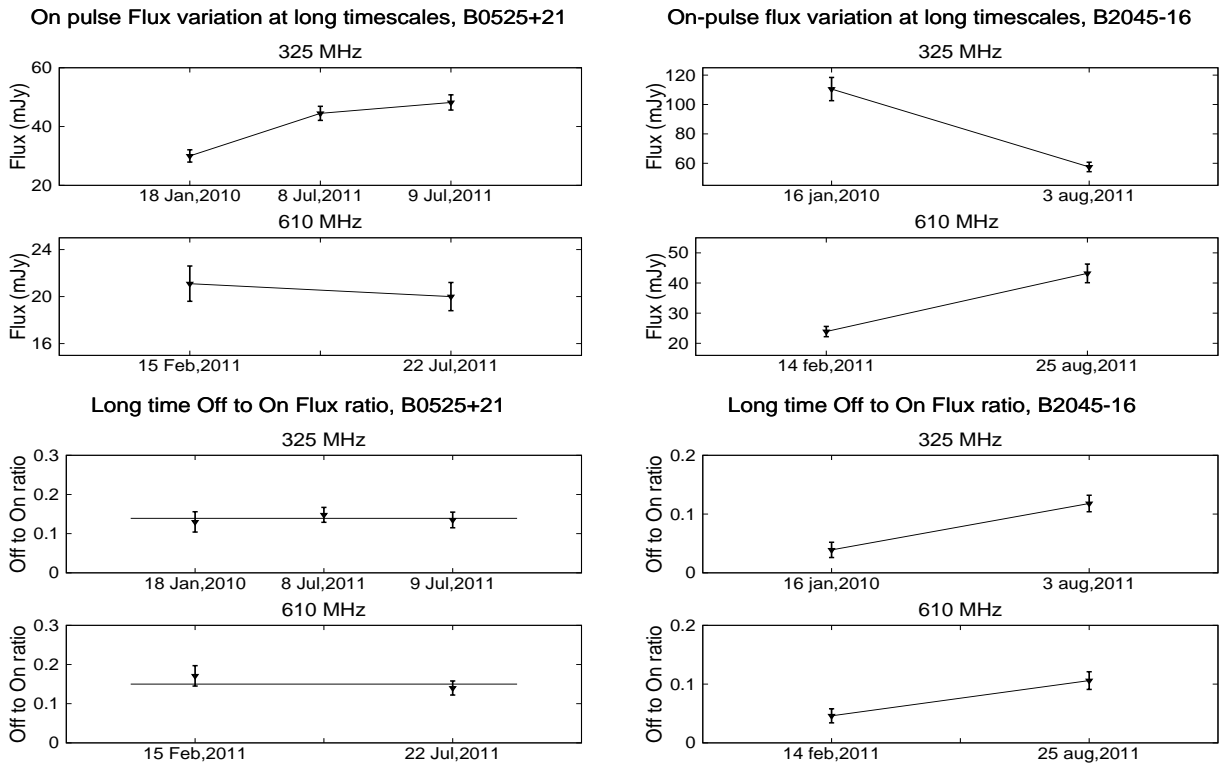


Fig. 4.— The plots show variation of the On-pulse flux and the Off-pulse to On-pulse flux ratio at large timescales. Each point in the plots is obtained averaging a single observing run lasting a few hours with the observations being distributed over several months. The pulsar B0525+21(left) show a constancy in the Off-pulse to On pulse flux ratio over these timescales, while for B2045-16(right) we observe an apparent variation.

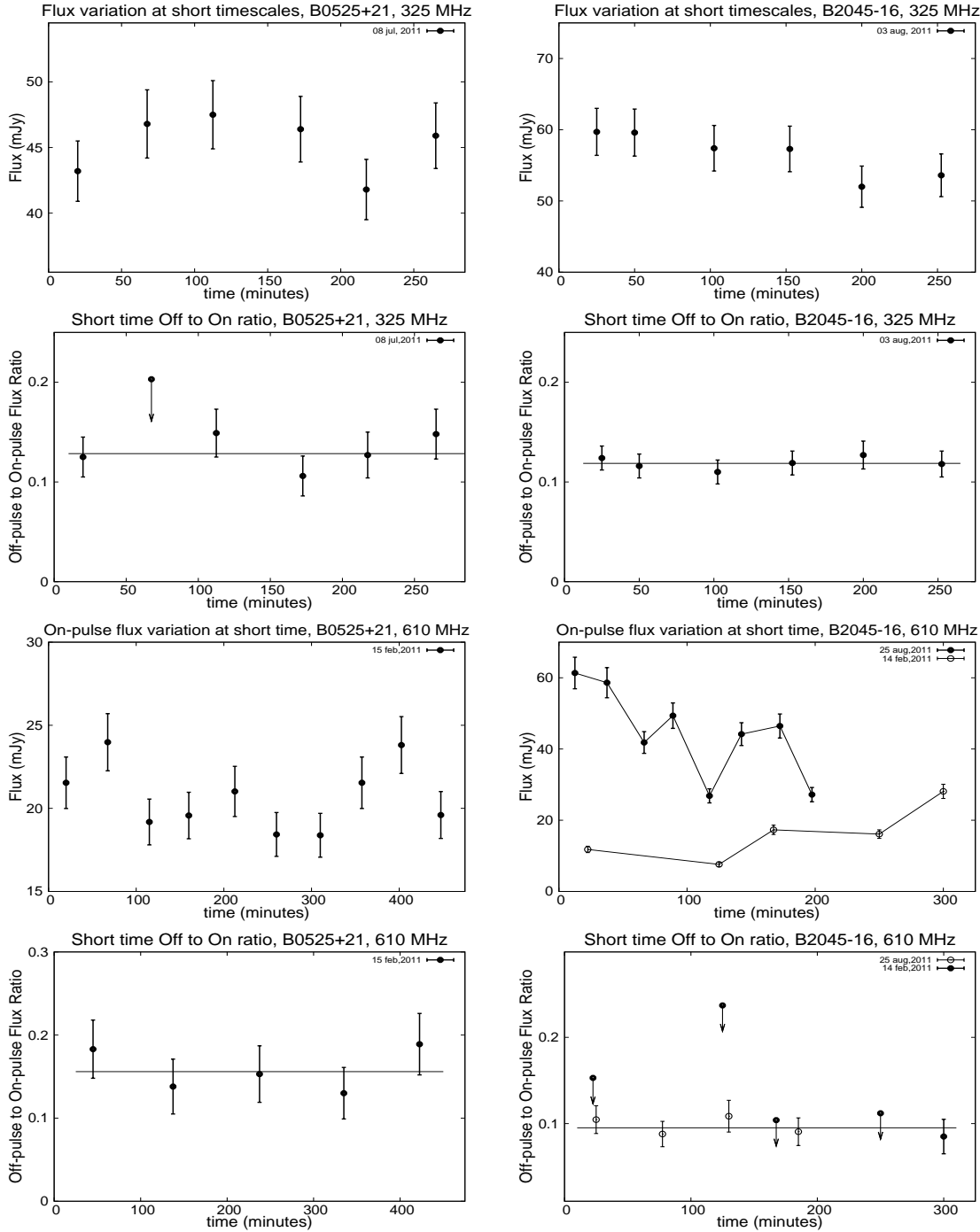


Fig. 5.— The plots show the variation of the On-pulse flux and the Off-pulse to On-pulse flux ratio at shorter timescales. The duration of a single observation spans several hours and the On- and Off-pulse fluxes were determined averaging 0.5 –1 hour at a time within a single observation. For the pulsar B0525+21 (left) the On-pulse flux varied at short timescales (several hours) within errors of measurements and the On-pulse to Off-pulse ratio remained constant at these timescales. In case of B2045-16(right) the On-pulse flux variations were once again within errors at 325 MHz with the Off-pulse to On-pulse flux ratio remaining constant. At 610 MHz the On-pulse flux showed large variations, however the Off-pulse to On-pulse flux ratio once again remained constant at short timescales for both the observations even though they go below detection level sometimes (arrows pointing downwards show upper limit of detection). This demonstrated both the long and short timescale constancy of the Off-pulse to On-pulse flux ratio for B2045-16 at 610 MHz.

sumably reflects the energy spectrum of the injected particles from the pulsar. In some older PWNe the spectrum might steepen somewhat, like in PWNe DA495 (Kothes et al. 2008) where the spectrum steepen to  $\alpha = -0.87$  above 1.3 GHz as a result of synchrotron aging. In contrast to PWNe the pulsed emission is the coherent radio emission arising due to relativistically streaming charged particles in strong magnetic field with the observed average  $\alpha \sim -1.8$  (Maron et al. 2000). Although in some examples the spectra might show breaks where  $\alpha$  is flatter for certain frequency range (like PSR B1952+29 has  $\alpha = -0.6$  between 400 MHz and 1.4 GHz, also see spectra of B2045-16, figure 6), mostly they are consistent with a steep power law spectra and a very low frequency turnover (around 100 MHz and below). Based on our current understanding, any emission originating close to the pulsar magnetosphere and with spectral index  $\alpha$  steeper than -0.9 is unlikely to be due to PWNe.

We set out to determine the spectral index of off-pulse emission based on our observations at 325 and 610 MHz. Spectral index determination requires robust flux estimates which is often difficult for pulsars. The measured pulsar flux is time variant due to both intrinsic and extraneous effects. The intrinsic variations occur in timescales of microseconds to several minutes manifesting as microstructures in single pulses, drifting subpulses, nulling, mode changing, etc. However the profile of a pulsar obtained averaging 2500–3000 pulses is relatively stable (Rathnasree & Rankin 1995). The pulsar flux is also affected by the inhomogeneities in the ISM leading to diffractive interstellar scintillations (DISS) and refractive interstellar scintillations (RISS). The DISS manifests as temporal flux variations with diffraction timescales ( $T_d$ ) ranging from seconds to minutes and also as decorrelation of flux with frequency known as decorrelation bandwidth ( $\Delta\nu_d$ ). The RISS shows variations at timescales ( $T_r$ ) of days to years with a flux modulation index ( $m_r$ ). These quantities scale with dispersion measure and frequency of observation typically as  $T_d \propto \nu^{1.2}$ ,  $\Delta\nu_d \propto \nu^{4.4}$ ,  $T_r \propto \nu^{-2.2}$  and  $m_r \propto \nu^{0.58}$  (Stinebring & Condon 1990). In order to determine the spectral index of the off-pulse emission it is imperative we understand its short and long term flux variations at each frequency.

**PSR B0525+21** has a dispersion measure of  $50.9 \text{ pc cm}^{-3}$  and its flux has been monitored at different frequencies for several years as reported in Lorimer et al. (1995) and Stinebring et al. (2000) (see fig 6 for the average flux at low frequencies). The long term averaging results in reduced contribution of RISS and DISS to the pulsar flux. Stinebring et al. (2000) quotes the scintillation parameters at our observing frequency 610 MHz as  $T_d \sim 70$  seconds,  $\Delta\nu_d \sim 230$  KHz,  $m_r \sim 0.32$ ,  $T_r \sim 4$  days. Using the scaling relations the equivalent quantities at 325 MHz are  $T_d \sim 33$  seconds,  $\Delta\nu_d \sim 15$  KHz,  $m_r \sim 0.22$ ,  $T_r \sim 16$  days.

Each of the GMRT observations for B0525+21 extends for about 6 to 8 hours and 16 MHz bandwidth at both 325 and 610 MHz. Any flux variations due to DISS will be greatly reduced over these scales. Due to RISS one expects 5% and 10% variation in flux over a single observing run at 325 MHz and 610 MHz respectively (these are comparable to the error in flux measurements and hence undetectable). In Table 1 the average On- and Off-pulse flux and the Off-pulse to On-pulse flux ratio during each observing session is reported. The long term flux change (about 55%) seen at 325 MHz (figure 4, 1<sup>st</sup> panel on left) is due to RISS, however the Off-pulse to On-pulse flux ratio remain constant both at 325 and 610 MHz (see figure 4, 2<sup>nd</sup> panel on left). The short term flux variations were determined by dividing a single observing session into shorter intervals (0.5 to 1 hour) and making images for each case. The On- and Off-pulse flux was measured for each interval and the Off-pulse to On-pulse flux ratio was calculated (see figure 5, panel on left). The short timescale flux variations were within the errors of measurement, as expected, and the Off-pulse to On-pulse flux ratio was also constant.

**B2045-16** has a dispersion measure of  $11.5 \text{ pc cm}^{-3}$  and its long term flux has been monitored at multiple frequencies by Stinebring & Condon (1990) and Lorimer et al. (1995). Based on daily flux measurements for 43 days, Stinebring & Condon (1990) quotes the scintillation parameters at 310 MHz (near our observing frequency of 325 MHz) as  $T_d \sim 63$  seconds,  $\Delta\nu_d \sim 288$  KHz,  $m_r \sim$



0.60 and  $T_r \sim 1.5$  days. Using the scaling relations the equivalent quantities at 610 MHz are  $T_d \sim 134$  seconds,  $\Delta\nu_d \sim 4$  MHz,  $m_r \sim 0.85$  and  $T_r \sim 0.5$  days.

The observations extended for 3 to 5 hours over 16 MHz bandwidth at both 325 and 610 MHz for each observing run. Any DISS related flux variations is expected to reduce due to averaging over time and frequency. However due to RISS we expect large flux variations of 110% and 40% over a single observing run at 610 and 325 MHz respectively. In table 1 the average On- and Off-pulse flux measurements and the Off-pulse to On-pulse flux ratios for each observation is quoted. The long term flux variations and Off-pulse to On-pulse flux ratio is shown in figure 4, right panel. The pulsar flux show variation in the flux values which are expected due to RISS, however the Off-pulse to On-pulse flux ratio also showed large variations at long timescales. The short timescale flux values were determined once again by dividing a single observing session into shorter intervals (0.5 to 1 hour) and making images for each case. The On-pulse flux at 610 MHz showed large variations in excess of 100% (see figure 5, 3<sup>rd</sup> panel on right), however the Off-pulse to On-pulse flux ratio, when detected, remained at constant level for the two observations separated by months (see figure 5, 4<sup>th</sup> panel on right). The apparent variation of the Off-pulse to On-pulse flux ratio at large timescales can be attributed to the fact that the Off-pulse was below detection limit for a large fraction of the observing run resulting in under estimation of the average Off-pulse flux over the entire observing run. At 325 MHz the short timescale measurements once again showed constant level Of Off-pulse to On-pulse flux ratio at short timescales for the observation on 3 august, 2011 (see figure 5, 2<sup>nd</sup> panel on right). The observation on 16 january, 2011 was affected by the telescope pointing 34' away from the pulsar resulting in increased noise levels at pulsar position thereby making the short interval studies impossible (the Off-pulse was undetected for the short interval studies due to higher noise levels). We conclude that despite the large variation of the On-pulse flux and the apparent variation of Off-pulse to On-pulse flux ratio at large timescales, the Off-pulse to On-pulse flux ratios remain constant at all timescales for this pulsar.

### 3.1. Refractive Scintillations: Upper limits to emission region.

The Off-pulse to On-pulse flux ratio as demonstrated above remains constant at all timescales for both the pulsars. This signifies that the timescales of refractive scintillations for the Off-pulse is similar to that of the main pulse, which readily puts a constraint on the size of the emitting region of the Off-pulse with respect to the On-pulse. If we assume a thin screen approximation for refractive scintillation, i.e, the refractive scintillations is due to a thin lens (0.001 – 0.005 fraction of the thickness of intervening medium) placed a fractional distance  $\beta$  ( $\beta = D_s/D$ , where  $D_s$  is separation between pulsar and lens and  $D$  the distance of pulsar from observer) from the pulsar, the refractive timescale is given as:

$$T_r = \frac{D_r}{V_{trans} \times (1 - \beta)} \quad (3)$$

where  $D_r$  is the diameter of the lens and  $V_{trans}$  the transverse velocity of the pulsar in the sky plane with respect to observer. The similar refractive timescales imply the On-pulse and Off-pulse emission is unresolved with respect to the lens putting an upper limit to emitting regions for the On- and Off-pulse with the maximum angular separation given as  $\theta_{max} \sim \lambda/D_r$ .

Using the known properties of the pulsars (table 2) and assuming the refractive lens lies mid way between the pulsar and observer ( $\beta = 0.5$ ) we calculate the diameter of the lens ( $D_r$ ) in each case using equation 3. This is further used to determine the upper limits to the angular size of the emitting region ( $\theta_{max}$ ). Finally the physical size of the maximum emitting region ( $R_{max}$ ) is calculated using  $\theta_{max}$  and distance to the pulsars (see table 2). The maximum emitting region (which is also the maximum separation between the On-pulse and Off-pulse emitting regions) is constrained to be a few microarcsec ( $\theta_{max}$ ). This further implies that the Off-pulse emission is constrained by the refractive scintillations to originate within an order of magnitude of the light cylinder radius ( $Pc/2\pi$ ). This as discussed previously is several orders of magnitude lower than the typical size of a PWN.

Table 2: The upper limits to emission region for Off-pulse emission using refractive scintillation.

Pulsar	period sec	dist kpc	$V_{trans}$ $\text{km s}^{-1}$	$T_r^{325}$ day	$T_r^{610}$ day	$Pc/2\pi$ km	$D_r^{325}$ km	$D_r^{610}$ km	$\theta_{max}^{325}$ ''	$\theta_{max}^{610}$ ''	$F_{max}^{325}$ km	$F_{max}^{610}$ km
B0525+21	3.746	2.28	229	16	4	$1.8 \times 10^5$	$1.6 \times 10^8$	$4.0 \times 10^7$	$1.2 \times 10^{-6}$	$2.5 \times 10^{-6}$	$4.1 \times 10^5$	$8.6 \times 10^5$
B2045-16	1.962	0.95	511	1.5	0.5	$0.9 \times 10^5$	$3.3 \times 10^7$	$1.1 \times 10^7$	$5.7 \times 10^{-6}$	$9.3 \times 10^{-6}$	$8.2 \times 10^5$	$13.2 \times 10^5$

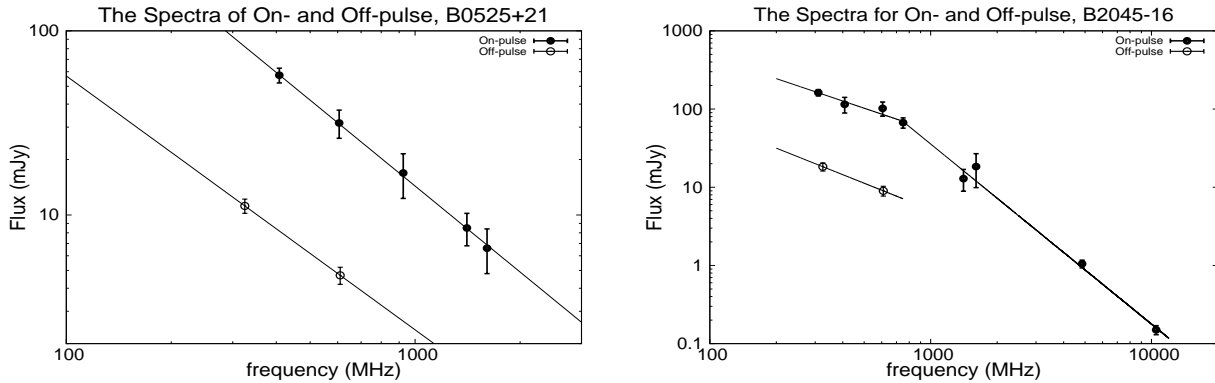


Fig. 6.— The plots show the On-pulse spectra and the derived Off-pulse spectra (using equation 4) for the two pulsars. For the pulsar B0525+21 (left) the On-pulse spectrum was determined between 300 MHz and 1.6 GHz by fitting a power law to the archival data (Maron et al. 2000; Lorimer et al. 1995). In case of B2045-16(right) the On-pulse spectrum was obtained between 300 MHz and 10 GHz. There is a break in spectrum around 750 MHz and two separate spectral index was calculated with values of -2.3 above 750 MHz which flattened to -0.95 at low frequencies.

Table 3: The spectral index for Off-pulse emission. The On-pulse spectra was determined by fitting the spectra for the flux from literature at low frequencies and using the Off- by On-pulse flux ratio to the Off-pulse spectra was calculated.

Pulsar	$\alpha_{ON}$	$(\frac{OFF}{On})_{325}$	$(\frac{OFF}{On})_{610}$	$\alpha_{OFF}$
B0525+21	$-1.5 \pm 0.1$	$0.139 \pm 0.012$	$0.150 \pm 0.015$	$-1.38 \pm 0.20$
B2045-16	$-0.95 \pm 0.12$	$0.118 \pm 0.014$	$0.106 \pm 0.015$	$-1.12 \pm 0.22$

### 3.2. Spectral index of On- and Off-pulse emission.

We have established that the Off-pulse to On-pulse flux ratio remain constant at all timescales. This enables us to determine the Off-pulse spectral index between 325 MHz and 610 MHz provided the On-pulse spectral index is known and both the emissions follow a power law spectrum. The off-pulse spectral index is given as:

$$\alpha_{OFF} = \alpha_{ON} + \frac{\log(\rho_1/\rho_2)}{\log(\nu_1/\nu_2)} \quad (4)$$

where  $\alpha_{OFF}$  and  $\alpha_{ON}$  are the Off-pulse and On-pulse spectral indices respectively and  $\rho$  the Off-pulse to On-pulse flux ratio at frequency  $\nu$ .

For the pulsar B0525+21 the spectrum between 400 MHz and 1.6 GHz is well known (Lorimer et al. 1995) shown in figure 6, which is well approximated by a single power law spectrum with spectral index  $-1.5$  (linear fit in fig 6). The Off-pulse spectral index is calculated using equation 4 and the Off-pulse to On-pulse flux ratios given in table 3. The off-pulse spectral index turns out to be  $-1.4$  which is pretty steep and comparable to the On-pulse spectral index.

For the pulsar B2045-16 we once again determine the spectrum from the literature (Lorimer et al. 1995 and Maron et al. 2000) over the frequency range 300 MHz to 10 GHz. In this case however the entire spectral range is not approximated by a single power law, with a clear break in the spectrum around 750 MHz (see figure 6). We determine the spectral index in this case by fitting two separate power laws above and below the break with spectral indices of  $-2.3$  for the high frequency range and  $-0.95$  for the low frequency regime. Our observations at 325 and 610 MHz lie in the low frequency range and we use this to calculate the spectral index of Off-pulse emission using equation 4 which turns out to be  $-1.1$ . This turns out to be steeper than the On-pulse spectra at the low frequency range.

## 4. Discussion

The discovery of radio emission in the Off-phase of two long period pulsars PSR B0525+21 and B2045-16 was reported in paper I. This emission, termed ‘Off-pulse emission’, occur far away from the typical main pulse in the pulsar profile

( $\geq 80^\circ$  from the peak of main pulse). The off-pulse emission unlike other emissions away from the main-pulse do not appear as temporal structures in the pulsar profile but rather as a constant background emission.<sup>1</sup>

In this paper we have focused on two important aspects:

(a) The off-pulse emission is unique in pulsars and it is important to ascertain that by no means the emission arises due to any instrumental effect or errors during data analysis. In section 2 we report detection of the off-pulse emission for B0525+21 and B2045-16 at widely separated times and different frequencies. We have conducted extensive tests and ruled out temporal leakage from a strong pulse as it passes through the GMRT receiver system as a possible source of Off-pulse emission. With these tests we are now absolutely certain that the off-pulse emission has an astronomical origin.

(b) The next important step was to establish through observational arguments the nature of Off-pulse emission. In section 3 we demonstrate that for PSR B0525+21 the Off-pulse to On-pulse flux ratio is constant at both 325 and 610 MHz, which in turn gives a spectral index  $\alpha_{OFF} \sim -1.4$ . We have also demonstrated that despite apparent variations in the long term Off-pulse to On-pulse flux ratio for the pulsar B2045-16, it actually remains constant at all timescales when the Off-pulse flux variations are taken into account. This once again allowed us to determine the spectral index of  $\alpha_{OFF} \sim -1.1$ . Based on the observed properties of refractive scintillation, we derived the radio emission region of the Off-pulse emission to have a maximum size of magnetospheric scale (see section 3.1). The steep spectral index coupled with a highly compact emission region make it highly unlikely for the Off-pulse emission to be a PWNe.

The Off-pulse emission appear to be a completely new and hitherto undetected magnetospheric emission from pulsars. The estimated brightness temperature of the Off-pulse emission is greater than  $10^{18}$  K, assuming the emission to originate at the light cylinder. This strongly sug-

<sup>1</sup>A more sensitive phase resolved study is currently underway where we aim at imaging each phase resolved bin to localize the off-pulse emission region.

gest a coherent radio emission process as the mechanism for explaining the Off-pulse emission which leads to the next important question as to where and how does this off-pulse coherent emission originate in the pulsar magnetosphere? Currently we do not have any good answers to these questions but there are a few likely possibilities that can be considered. The basic pulsar models suggest that the power from the rotational energy in a neutron star is tapped and converted into the observed radiation. The rotating magnetic field of the neutron star acts like a unipolar inductor, creating high electric fields around the neutron star where charged particles are accelerated to relativistic velocities along the open field lines. This eventually leads to the pulsar radiation. A large number of models exist which try to establish the location of the charge accelerating regions and suggest physical mechanisms that can excite the coherent radio emission in pulsars. However here we will not go into the details of any of these models, but would like to point out as why finding the location of the emission region in the pulsar magnetosphere is central in unravelling the origin of the Off-pulse emission.

In most pulsar theories the radio emission is excited due to development of plasma instabilities in the outflowing plasma. The main pulse emission arises around 500 km above the neutron star surface (Blaskiewicz et al. 1991; Rankin 1993; Kijak & Gil 1998; Krzeszowski et al. 2009). At these heights the magnetic field is very strong, and the relativistic charged plasma particles are forced to move along the curved magnetic field lines. Here the well known two-stream plasma instability naturally generates langmuir plasma waves. If the plasma is subjected to a non-stationary flow, then it leads to the modulational instability of Langmuir waves which results in formation of relativistic charged solitons capable of emitting coherent curvature radiation (Melikidze et al. 2000; Gil et al. 2004; Mitra et al. 2009). The Off-pulse emission on the other hand lies in the region outside the main pulse, and currently we are not certain about its exact location. For the emission to originate from open field lines, the location needs to be above the main pulse in regions where the open dipolar magnetic field lines diverge. As the pulsar rotates, this divergent region above the main pulse is sampled by the

observer as the Off-pulse emission. The other well known maser type plasma instability that can give rise to the coherent emission are the cyclotron– cherenkov or cherenkov drift instability (Kazbegi et al. 1987; Kazbegi et al. 1991). The instabilities are due to the interaction of the fast particles of the primary beam with the normal modes of the electron-positron plasma. These instabilities are known to operate close to the light cylinder and could be a viable source of Off-pulse emission.

There might be other possible origin of the Off-pulse emission which we will need to evaluate and understand in the future, however it is clear that this newly found Off-pulse emission from low energetic slowly rotating neutron stars provide important clues in understanding the physical phenomenon operating in the pulsar magnetosphere.

## 5. Acknowledgments

We would like to thank Jayanta Roy for developing the 128 millisecond interferometric mode of the GMRT software backend(GSB) which were used as a part of these observations. We would also like to thank Navnath Shinde, Sweta Gupta, Ajay Vishwakarm, Ajit Kumar and other members of the GMRT engineering team for developing the pulsed noise source used in our studies. We thank the staff of the GMRT that made these observations possible. GMRT is run by the National Centre for Radio Astrophysics of the Tata Institute of Fundamental Research.

*Facility:* GMRT.

## REFERENCES

- Basu, R., Athreya, R., Mitra D. 2011, ApJ, 728, 157
- Blaskiewicz, M.; Cordes, J.M.; Wasserman, I. 1991, ApJ, 370, 643
- Frail, D.A., Scharringhausen, B.R. 1997, ApJ, 480, 364
- Gaensler, B.M.; Slane, P.O. 2006, ARA&A, 44, 17
- Goldreich, P., Julian, W. H. 1969, ApJ, 157, 869
- Gil, J.; Lyubarsky, Y.; Melikidze, G.I. 2004, ApJ, 600, 872

- Kazbegi, A.Z.; Machabeli, G.Z.; Melikidze, G.I.  
1987, AuJPh, 40, 755
- Kazbegi, A.Z.; Machabeli, G.Z.; Melikidze, G.I.  
1991, MNRAS, 253, 377
- Kijak, J.; Gil, J. 1998, MNRAS, 299, 855
- Kothes, R.; Landecker, T.L.; Reich, W.; Safi-  
Harb, S.; Arzoumanian, Z. 2008, ApJ, 687, 516
- Krzeszowski, K.; Mitra, D.; Gupta, Y.; Kijak, J.;  
Gil, J.; Acharyya, A. 2009, MNRAS, 393, 1617
- Lorimer, D.R., Yates, J.A., Lyne, A.G., Gould,  
D.M. 1995, MNRAS, 273, 411
- Maron, O.; Kijak, J.; Kramer, M.; Wielebinski, R.  
2000, A&AS, 147, 195
- Melikidze, G.I.; Gil, J.A.; Pataraya, A.D. 2000,  
ApJ, 544, 1081
- Mitra, D.; Gil, J.; Melikidze, G.I. 2009, ApJ, 696,  
141
- Rankin, J.M. 1993, ApJ, 405, 285
- Rathnasree, N., Rankin, J. M. 1995, ApJ, 452, 814
- Rickett, B.J. 1990, ARA&A, 28, 561
- Ruderman, M. A., Sutherland, P. G. 1975, ApJ,  
196, 51
- Stinebring, D.R., Condon, J.J, 1990, ApJ, 352,  
207
- Stinebring, D.R., Smirnova T.V., Hankins, T.H.,  
Hovis, J.S., Kaspi, V.M., Kempner, J.C., Myers  
E., Nice D.J. 2000, ApJ, 539, 300
- Thomson, A.R., Moran, J.M., Swenson G.W.  
1986, Interferometry and Synthesis in Radio  
Astronomy (Wiley Interscience, New York).
- Weiler, K.W.; Sramek, R.A., 1988, ARA&A, 26,  
295